

Novel application of ceramic precursors for the fabrication of composites

Andreas Herzog^{a,*}, Maik Thünemann^a, Ulrich Vogt^a, Olivier Beffort^b

^a *Laboratory of High Performance Ceramics, Swiss Federal Laboratories for Materials Testing and Research, CH 8600 Duebendorf, Ueberlandstr. 129, Switzerland*

^b *Laboratory of Materials Technology, Swiss Federal Laboratories for Materials Testing and Research, CH 3602 Thun, Feuerwerkerstr. 39, Switzerland*

Available online 27 September 2004

Abstract

Preceramic polymers are enabling the development of a variety of advanced shaping methods which, in turn, make possible new and cost-effective approaches for the fabrication of composite materials. This opens new perspectives for the mass production of composites which might, for example, be used in cost-sensitive areas of application in the machine and automobile industries. In two examples it will be shown how preceramic polymers can be used to obtain both metal matrix composites (MMC) and ceramic matrix composites (CMC). Their properties will be discussed in particular with respect to the usage of a preceramic polymer.

The first example shows an approach to manufacturing short-fibre-reinforced CMCs by means of a plastic forming technique which involves mixing of either carbon or SiC fibres, ceramic fillers and a viscous ceramic precursor. The precursor permits a fibre-reinforced ceramic with a low porosity to be obtained. The role of the precursor in the whole process and the resulting material properties will be discussed.

The second example shows a method for fabricating porous SiC ceramic preforms which are subsequently infiltrated with aluminium to form a MMC. By using the precursor route, a machinable preform with tailored porosity can be produced. Correlations between precursor, preform and MMC properties will be drawn.

© 2004 Published by Elsevier Ltd.

Keywords: Silicon carbide; Pyrolysis; Nitridation; Quasiductile behaviour; Precursor organic

1. Experimental

1.1. CMC processing

Either C-fibres (Sigrafil C25, SGL Carbon) or SiC fibres (Tyranno ZMI, UBE Ind.), preceramic polymer (Siloxane MK, Wacker) and silicon (Bayer) were mixed for 2 h in a warm kneader (Werner&Pfleiderer, Luk 8.0). Subsequently the material was cooled down, granulated and formed by a warm pressing process at 150 °C (WirtzBuehler, Simplimet 2000). The pressed tablets (diameter 50 mm) were cured in air with a low heating ramp of 1 °C/h up to 235 °C and afterwards cut by a diamond saw into bars of 4 mm × 8 mm × 20–50 mm. The examined compositions are summarised in Table 1.

Pyrolysis (Program T0 below) was carried out in flowing nitrogen (purity 99.999), followed by nitridation (T1) under 0.1 MPa nitrogen:

T0:RT → 160 °C (160 °C/h) → 750 °C (20.4 °C/h) → 900 °C (42.8 °C/h)

T1:RT → 1170 °C (180 °C/h) → 1400 °C (9.6 °C/h), 24 h holding, $p_{N_2} = 0.1$ MPa

1.2. MMC processing

In order to coat the silicon carbide particles, siloxane was dissolved in 2-propanol, mixed with the silicon carbide powder (F100, Saint Gobain) and dried carefully in a vacuum rotation evaporator (Rotavapor R-134, Büchi) at 40 °C and 80 mbar. After sieving the polymer-coated and dried SiC particles, a powder with good flowability was obtained. The coated powder was warm pressed (38 MPa, 10 min) to tablets

* Corresponding author. Tel.: +49 41 1 823 4817; fax: +49 41 1 823 4150.
E-mail address: andreas.herzog@empa.ch (A. Herzog).

Table 1
Specimen composition

Specimen	Fibre	Composition (wt.%)			Composition (vol.%)		
		Fibre	Si	MK	Fibre	Si	MK
A0	None	0	71.5	28.5	0	58.3	41.7
A2	Carbon	30	41.5	28.5	29.6	31.6	38.9
C2	SiC	37.5	36.7	25.8	29.6	31.1	39.2

($\varnothing = 40$ mm, $h = 2$ mm) at the curing temperature of the polymer. As curing during pressing was insufficient, a pre-curing step was subsequently incorporated. The tablets were pyrolysed with $1^\circ\text{C}/\text{min}$ to 1000°C in nitrogen atmosphere with 3 h holding time in order to convert the polymer into the ceramic phase. Tablets with a polymer content between 2.5 and 10 wt.% relative to SiC (5 vol.% to 20 vol.%, respectively) content were prepared.

Pressed and pyrolysed tablets were infiltrated by squeeze casting with aluminium 99.99%. For the exact squeeze casting procedure, refer to Long.¹

1.3. Examination

Specimens were characterised by optical microscopy (Zeiss) and electron microscopy (Joel JSM 6300F). Porosity was measured by a mercury porosimeter (Micromeritics, Autopore II 9220). Changes in length were monitored by dilatometry (402E, Netzsch), where samples were heated at $5^\circ\text{C}/\text{min}$ up to 1170°C and $2^\circ\text{C}/\text{min}$ up to 1400°C and finally held 10 h.

The phase composition was studied by X-ray powder diffraction (Philips PW 1710) in combination with external standard for Si_3N_4 and Si_2ON_2 . The SiC content was determined by a carbon detector (CSA 2003, Leybold-Heraeus), and free silicon by the gas volumetric method according to DIN 51075. Free carbon content was determined by oxidation for 1 h at 1000°C .

The strength of CMC bars was measured according to EN843-1 with the 3-point bending test. Strength of preform and MMC tablets ($\varnothing = 40$ mm, $h = 2$ mm) was assessed using a double-ring-bending test (diameter of outer ring 36 mm, inner ring 12 mm) on a universal testing machine (Zwick) in accordance to DIN 52292-1, 1984.

2. Results

2.1. Pyrolysis

Pyrolysis of the pure preceramic polymer shows a ceramic yield of 85%. In combination with metals like silicon, as is the case during CMC production, the ceramic yield is increasing by 5%. According to Erny,² dissociation and adsorption of gaseous pyrolysis products such as H_2 and CH_x on the surface of the reactive filler phase (silicon) is responsible for this increase. For passive SiC in the case of MMC production, such behaviour is not found and the ceramic yield of the precursor after pyrolysis is equal to that of the precursor itself.

The significant amounts of preceramic polymer used for CMC production cause a significant linear shrinkage during pyrolysis (Fig. 1). During this process, porosity remains constant in the range of 3 vol.%. It can be concluded that the volume decrease caused during pyrolysis of the preceramic polymer (weight loss of 15 wt.% and a density increase by 77% from 1.3 to $2.3\text{ g}/\text{cm}^3$) is totally compensated by the shrinkage. However, preferred fibre distributions hinder the even shrinkage of the matrix, causing so-called differential shrinkage. This can cause stresses over 50 MPa ³ in the material which exceed the inherent strength of the precursor during pyrolysis. Consequently, cracks form in the material which seriously impairs the strength of the finished materials after nitridation. Fig. 2 shows a typical micrograph of pyrolysed CMC A2 with an equal distribution of fibres and matrix ingredients.

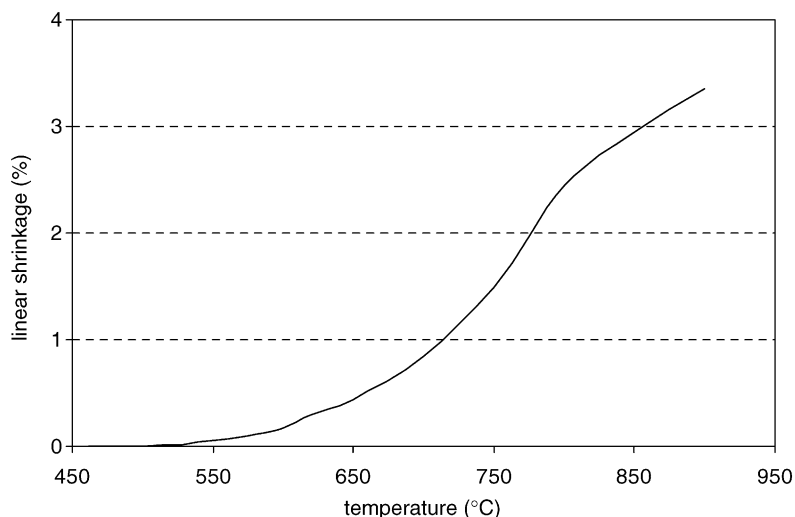


Fig. 1. Shrinkage of C fibre CMC, A2, during pyrolysis.

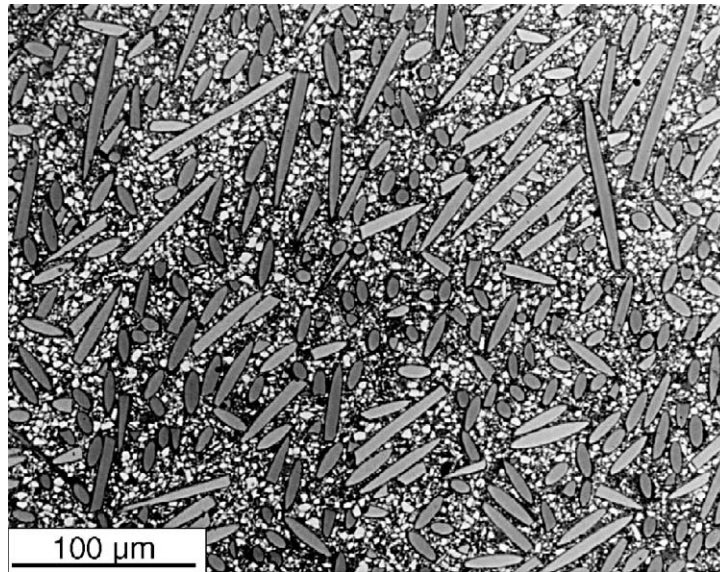


Fig. 2. Pyrolysed C fibre CMC, A2, white parts = silicon, optical microscope.

The smaller amounts of polymer used for MMC production as well as the porous structure of the preform itself result in almost negligible shrinkage (approx. one order of magnitude lower than observed for CMC) during pyrolysis in this system. Porosity remains almost constant in comparison to the state before pyrolysis and lies in the range of 41 vol.% (2.5 wt.% precursor) and 30 vol.% (10 wt.% precursor). Pore diameters are determined by the primary particle size and are in the range between 30 and 40 μm . After pyrolysis, the biaxial strength depends on the polymer content and porosity and typically lies in the range of 2–4 MPa which is sufficient for further handling. As pointed out recently by Thünemann et al.,⁴ the strength increases with increasing precursor content and decreasing porosity. A fracture surface of a pyrolysed preform shows polymer-coated SiC grains (Fig. 3). The coating thickness is in the order of 1–2 μm , but polymer also tends to collect in the voids between the particles. Cracking of the coating is caused by extensive shrinkage of the polymer during pyrolysis ($\Delta V = 50$ vol.%).

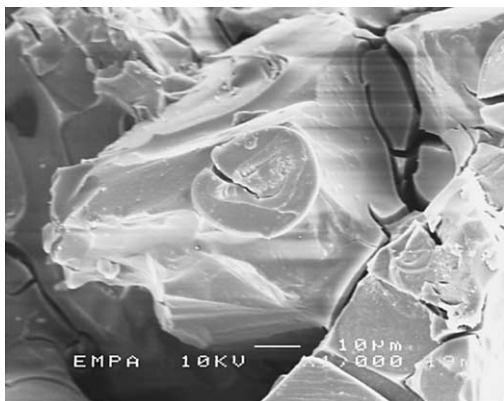
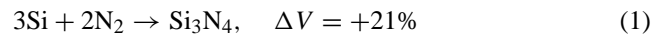


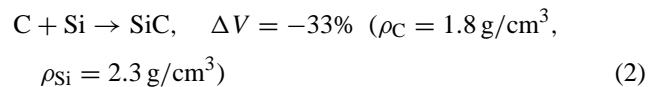
Fig. 3. Pyrolysed MMC preform, SEM.

2.2. Nitridation (CMC only)

Pyrolysis of the CMC preforms is followed by nitridation. Once the nitridation temperature ($T > 1350$ °C) is reached, volume expansion of the silicon nitridation starts (Eq. (1)) and shrinkage stops.



Generally, the amount of expansion due to nitridation depends on the silicon content of the specimens, i.e. the degree of expansion increases with increasing silicon content. However, not only nitride phases are developed during nitridation (Fig. 5). Approximately 1/3 of the introduced C-fibres are consumed by reaction with free Si to form SiC (Eq. (2)). Once a first layer of SiC is formed at the fibre surface, continued SiC formation is dictated by the diffusion coefficient of silicon through the SiC layer.^{3,5} Formation of SiC is enhanced by cracks within the SiC layer which provide a preferred diffusion path. SiC-formation is in competition with the nitridation reaction as both start in a similar temperature range with same thermodynamic likelihood. As SiC formation causes a volume decrease (Eq. (2)), a significant porosity increase (3/23 vol.%) is observed in CMC A2 instead of the desired decrease by volume expansion by nitridation.



SiC formation between the matrix silicon and the carbon fibres takes place at the interface of the two phases, causing a shell-like structure. Different expansion coefficients of the SiC reaction layer ($\alpha = 5.8 \times 10^{-6} \text{ }^\circ\text{C}^{-1}$) and the carbon fibres ($\alpha_{\text{rad}} = 8 \times 10^{-6} \text{ }^\circ\text{C}^{-1}$) cause tension within the interface and consequently separation between fibres and the SiC shells takes place during cooling. The small interface

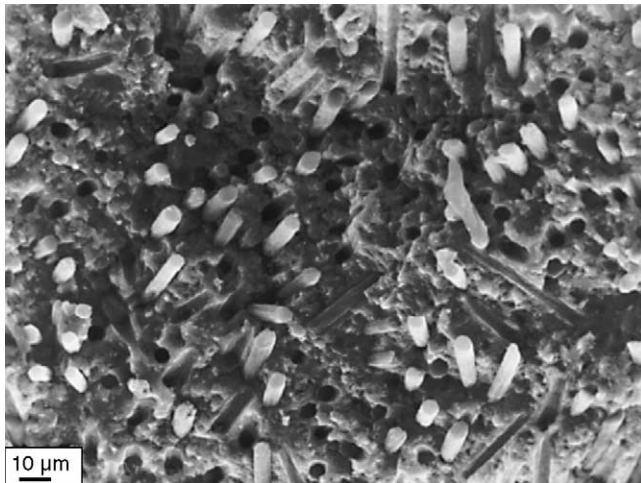


Fig. 4. Fracture surface of nitrated A2, fibre pullout.

gap allows fibre pull out and crack deflection during fracture and can be observed in fracture surface (Fig. 4). Both processes are a prerequisite for quasiductile behaviour of CMCs.

The nitridation behaviour of the SiC-reinforced sample C2 is different from the C-fibre CMC A2. As no volume-decreasing SiC formation takes place in sample C2, the porosity increase is smaller (3/12 vol.%) than in A2. This has consequences for nitridation efficiency and fibre pullout. Nitridation speed and efficiency decrease for C2 in comparison to A2 since a 3D pore channel system is a prerequisite for N₂ transport. Thus full nitridation does not develop perfectly. As a result, nitridation is not carried out completely in the same time as observed for A2. Consequently after nitridation, the phase composition still shows a silicon content of 7 wt.% and less nitride phase (Fig. 5). It has been already pointed out by the authors that full nitridation of samples containing SiC-fibres can be reached by either Si₃N₄ seeding of the matrix and/or increasing the

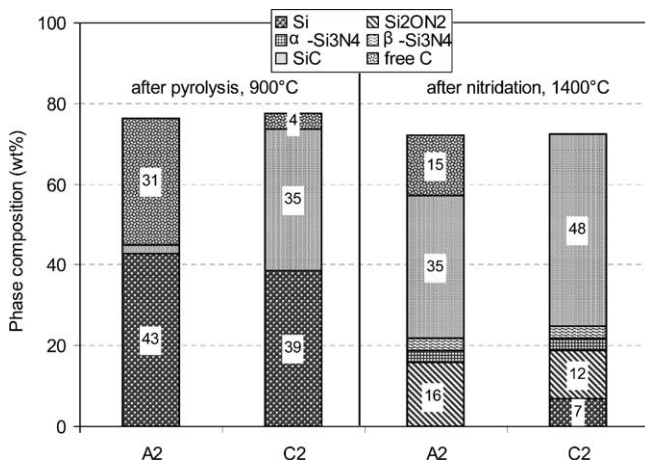


Fig. 5. Phase composition of A2 (C fibre) and C2 (SiC fibre) after pyrolysis and nitridation (missing part to 100% due to amorphous phase caused by pyrolysis products of precursor).

pressure during nitridation.⁶ As no interlayer between fibre and matrix forms during nitridation in C2 no fibre pullout is observed.

2.3. Metal infiltration (MMC only)

Pyrolysis of the MMC preforms is followed by aluminium infiltration. During this infiltration there is a thermodynamic probability that Al₄C₃ forms at the SiC–Al interface. Belfort et al.⁷ have discussed that development of such a phase during the squeeze casting process is suppressed by kinetic hindrance caused by quick solidification and saturation of aluminium with silicon in the SiC–Al interface region. A micrograph showing a typical final MMC microstructure is shown in Fig. 6.

The homogeneity of the polymer coating can be influenced by the processing parameters and seems to have an impact on the mechanical behaviour of the MMC (Fig. 7). A homogeneous coating on the primary SiC particles forms a preform with a Table 3D ceramic network. Consequently, after infiltration, the metal and ceramic phases form an interpenetrating network which is most favourable for MMCs.⁸ Such MMCs exhibit more ceramic-like behaviour, i.e. the composite is stiffer and exhibits brittle fracture behaviour. Inhomogeneous coatings cause a behaviour of the MMC which reflects the behaviour of loose particles embedded in a metal matrix, i.e. the stable 3D ceramic network does not form. This means the fracture behaviour is mainly ruled by the 3D metal phase and therefore the composite is more ductile, but less stiff and lower in strength.

Double ring strength testing revealed a fracture strength of 480 MPa for samples with a homogeneous coating and 292 MPa for samples with an inhomogeneous coating. Comparison with literature data⁷ shows a strength of 470 MPa for a loose SiC-particle–aluminium MMC in four-point bending. For comparison with four-point bending results, a factor of 1.17 must be applied to the double ring strength to account for the larger volume tested in the double ring test. The factor is calculated for a Weibull $m = 10$ using Eq. (3):

$$\frac{\sigma_R}{\sigma_F} = \left(\frac{V_F}{V_R} \right)^{1/m}, \quad R : \text{double ring}, F : \text{four-point bending} \quad (3)$$

Calculating the four-point bending strengths of MMCs possessing a homogeneous coating accordingly gives values up to 565 MPa.

3. Discussion

Both types of composite demonstrate that the preceramic polymer has several functions in the production process. In both cases the preceramic polymer enables forming of the material and subsequent machining of the green body. As such, conventional techniques and devices common to the

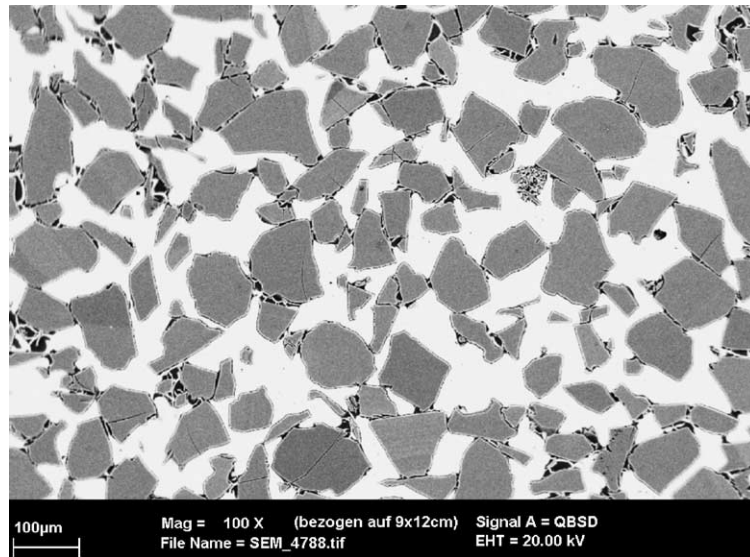


Fig. 6. Al/SiC MMC: white, Al; grey, SiC; black, precursor.

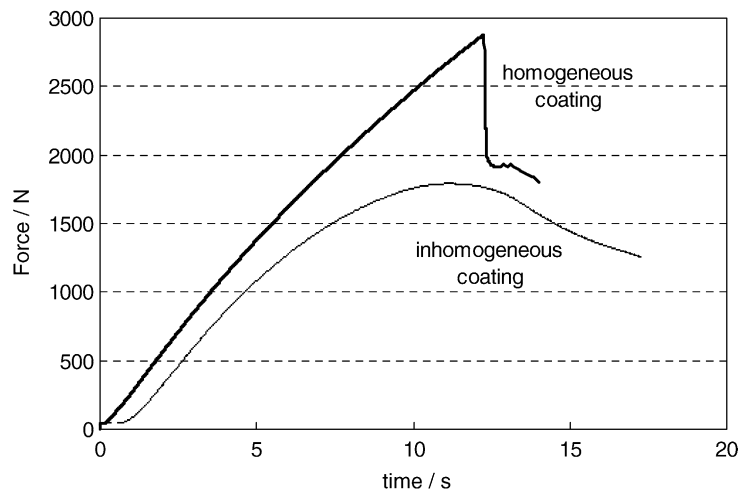


Fig. 7. Double ring test on Al/SiC MMC.

plastics industry, including the well-known mass production technique of injection moulding, can be used for the fabrication of these composites.

Regarding the fabrication of CMCs, the use of a fusible, viscous precursor allows the formation of a homogeneous fibre-silicon mixture with very low porosity. Here the polymer acts as a pore filler and space holder of fibres. For specimens without fibres, this function is already known.⁹ Compression and fixing of fibres by the binding forces of the precursor phase allows the fibre volume in the CMC to be increased. Additionally, the method avoids the increase in porosity which is normally reported for fibre–powder mixtures.¹⁰

In particular for MMCs, the dependence shown above between porosity, polymer content and strength allows the preform properties to be tailored to the demands of MMC manufacturers.

The extensive volume shrinkage during pyrolysis of the precursor causes problems to both MMC and CMC fabrication by this method.

In the MMCs, cracking of the precursor coating on the SiC particles occurs. However, point contacts between coated SiC particles impart sufficient strength to the preform to enable further handling and infiltration of the preform. It is assumed that cracking of the precursor layer causes a partial peel off of the coating, thereby forming a gap between SiC particles and the precursor coating layer. During infiltration, metal penetrates into this gap and direct bonding between the SiC particles and the metal will be possible. Additionally, bonding in the MMC may also occur between the metal and the preceramic layer, which in turn bonds to the underlying SiC particle. Consequently, both, direct SiC–metal bonding and indirect SiC–preceramic–metal bonding contribute to the strength of the MMC structure. Negligible shrinkage

of the external dimensions of the preforms during pyrolysis allows near net shape manufacturing of porous preforms without distortion.

In the CMC case, the volume shrinkage of the polymer causes volume shrinkage of the composite on a similar scale. Differential shrinkage due to preferred fibre orientation causes cracking in the material and limits mechanical strength to 50 MPa (three-point bending), even after nitridation. For the moment this limits the realisation and technical application of such a material. In future, efforts should be made to minimise in particular the problem of differential shrinkage. This can be approached by applying an interfacial layer between the fibres and the matrix which enables internal stresses to be relieved. This, in turn, may allow unhindered shrinkage of the matrix as well as decrease differential shrinkage and thus avoid cracking. Chih and Fu¹¹ has controlled the interface by a applying SiO₂ coating and has demonstrated a reduction of the internal stresses. Avoiding the more central problem of differential shrinkage, fibre orientation, seems more difficult and may in future demand major changes in production technique.

References

1. Long, S., Beffort, O., Moret, G. and Thevoz, P., *Aluminium 1/2*, Vol 76, 2000, pp. 82–89.
2. Erny, T., Seibold, M., Jarchow, O. and Greil, P., *J. Am. Ceram. Soc.*, 1993, **76**(1), 207ff.
3. Herzog, A., Manufacturing and properties of short fibre reinforced reaction bonded silicon nitride. Dissertation University Erlangen Nuernberg in German only, 2002. VDI Fortschrittsberichte Reihe 5 Nr. 668, VDI Verlag Düsseldorf.
4. Thünemann, M., Herzog, A., Vogt, U. and Beffort, M., *Adv. Eng. Mater.*, 2004, **6**(3), 167–172.
5. Gadow, R., *Keramische Zeitschrift*, 1988, **6**, 76ff.
6. Herzog, A., Vogt, U., *Ceramic Engineering and Science Proceedings, 26th Annual International Conference on Advanced Ceramics and Composites*, Vol 23(3), ed. H. Lin and M. Singh, 2002, pp. 19–26.
7. Beffort, O., Kübler, J., Cayron, C. and Buffat, P. A., Verbundwerkstoffe, 14. In *Symposium Verbundwerkstoffe und Werkstoffverbunde, DGM*. Wiley-VCH, H.P. Degischer, Verlag, 2003, pp. 61–66.
8. Claussen, N., Knechtel, M., Prielipp, H. and Rödel, J., *cfi/Ber. DKG*, Vol 71, No 6, 1994, p. 301.
9. Kleber, S. and Weiss, H., *J. Eur. Ceram. Soc.*, 1992, **10**, 205ff.
10. Milewski, J., *Adv. Ceram. Mater.*, 1986, **1**(1), 36ff.
11. Chih, C.-C. and Fu, S.-Y., *J. Mater. Sci.*, 1994, **29**(12), 3215ff.